J|A|C|S ARTICLES

Published on Web 01/23/2009

Redox Actuation of a Microcantilever Driven by a Self-Assembled Ferrocenylundecanethiolate Monolayer: An Investigation of the Origin of the Micromechanical Motion and Surface Stress

Lana L. Norman and Antonella Badia*

FQRNT Center for Self-Assembled Chemical Structures, Regroupement québécois sur les matériaux de pointe, and Department of Chemistry, Université de Montréal, C.P. 6128 succursale Centre-ville, Montréal, QC H3C 3J7 Canada

Received October 26, 2008; E-mail: antonella.badia@umontreal.ca

Abstract: The electrochemically induced motion of free-standing microcantilevers is attracting interest as micro/nanoactuators and robotic devices. The development and implementation of these cantilever-based actuating technologies requires a molecular-level understanding of the origin of the surface stress that causes the cantilever to bend. Here, we report a detailed study of the electroactuation dynamics of gold-coated microcantilevers modified with a model, redox-active ferrocenylundecanethiolate self-assembled monolayer ($FcC_{11}SAu$ SAM). The microcantilever transducer enabled the observation of the redox transformation of the surface-confined ferrocene. Oxidation of the $FcC_{11}SAu$ SAM in perchlorate electrolyte generated a compressive surface stress change of -0.20 ± 0.04 N m^{-1}, and cantilever deflections ranging from $\sim$0.8 μm to $\sim$60 nm for spring constants between $\sim$0.01 and $\sim$0.8 N m^{-1}. A comparison of the charge-normalized surface stress of the $FcC_{11}SAu$ cantilever with values published for the electrochemical oxidation of polyaniline- and polypyrrole-coated cantilevers reveals a striking 10- to 100-fold greater stress for the monomolecular $FcC_{11}SAu$ system compared to the conducting polymer multilayers used for electroactuation. The larger stress change observed for the $FcC_{11}SAu$ microcantilever is attributable to steric constraints in the close-packed $FcC_{11}SAu$ SAM and an efficient coupling between the chemisorbed $FcC_{11}S-$ monolayer and the Au-coated microcantilever transducer (vs physisorbed conducting polymers). The microcantilever deflection vs quantity of electrogenerated ferrocenium obtained in cyclic voltammetry and potential step/hold experiments, as well as the surface stress changes obtained for mixed $FcC_{11}S-/C_{11}SAu$ SAMs containing different populations of clustered vs isolated ferrocenes, have permitted us to establish the molecular basis of stress generation. Our results strongly suggest that the redox-induced deflection of a $FcC_{11}SAu$ microcantilever is caused by a monolayer volume expansion resulting from collective reorientational motions induced by the complexation of perchlorate ions to the surface-immobilized ferroceniums. The cantilever responds to the lateral pressure exerted by an ensemble of reorienting ferrocenium-bearing alkylthiolates upon each other rather than individual anion pairing events. This finding has general implications for using SAM-modified microcantilevers as (bio)sensors because it indicates that the cantilever responds to collective in-plane molecular interactions rather than reporting individual (bio)chemical events.

Introduction

This article reports the reversible potential-controlled actuation and surface stress properties of free-standing gold-coated microcantilevers functionalized with a redox-active self-assembled monolayer (SAM). Our results show that the electrochemical transformation of a redox (ferrocene) moiety confined to the surface of a chemisorbed organic film can induce a vertical bending or deflection approaching the micrometer scale for a very flexible microcantilever. The surface stress change per charge density for the *monomolecular* redox-active SAM is $\sim$10- to 100-fold greater in magnitude than that of conducting macromolecular systems used for electroactuation. The work reported herein expands the types of organic coatings than can be used for mechanical actuation and provides fundamental insights into the response mechanism of microcantilever-based sensing and actuating technologies.

The deflection of micromechanical cantilevers used as imaging probes and picoNewton force sensors in atomic force microscopy (AFM) is generating growing interest for label-free (bio)chemical sensing and mechanical actuation.[1−11] To date, a variety of biomolecular interactions and chemical reactions have been translated into a nanoscale deflection of the cantilever: DNA hybridization,[12−21] ligand−receptor binding,[12,22−24]

(1) Lang, H. P.; Hegner, M.; Gerber, C. *Mater. Today* **2005**, *8*, 30–36.
(2) Raiteri, R.; Grattarola, M.; Butt, H.-J.; Skládal, P. *Sens. Actuators, B* **2001**, *79*, 115–126.
(3) Sepaniak, M.; Datskos, P.; Lavrik, N.; Tipple, C. *Anal. Chem.* **2002**, *74*, 568A–575A.
(4) Hansen, K. M.; Thundat, T. *Methods* **2005**, *37*, 57–64.
(5) Lang, H. P.; Baller, M. K.; Berger, R.; Gerber, Ch.; Gimzewski, J. K.; Battiston, F. M.; Fornaro, P.; Ramseyer, J. P.; Meyer, E.; Güntherodt, H. J. *Anal. Chim. Acta* **1999**, *393*, 59–65.
(6) Ziegler, C. *Anal. Bioanal. Chem.* **2004**, *379*, 946–959.

 10.1021/ja808400s CCC: $40.75

protein−protein recognition,[12,17,25,26] cell adhesion,[27,28] alkanethiol self-assembly,[29−34] protonation/deprotonation of acid/base groups,[35−39] metal ion complexation,[40−43] underpotential metal deposition,[44−48] doping/dedoping of conducting polymers,[49,50] and the swelling/collapse of polyelectrolyte brushes.[51−55] The basic principle is that a chemical or physical event occurring at the functionalized surface of one side of the cantilever generates a surface stress difference (between the active functionalized and passive nonfunctionalized sides) that causes the cantilever to bend away from its resting position. To activate one side of the silicon or silicon nitride cantilever, its surface is usually coated with a thin metal film and/or modified with a (bio)organic layer. The cantilever deflection can be monitored in real-time with angstrom sensitivity via a laser beam reflected from the free end of the microcantilever onto a position-sensitive detector (PSD).[56] The deflection can be converted to a differential surface stress through a modified form of Stoney's equation.[57−60] It is well-known that for isotropic materials, a compressive surface stress change yields an increase in the surface area, while a tensile stress leads to a decrease in area. In the case of microcantilevers, the compressive stress arises from repulsive, in-plane molecular interactions and results in a deflection away from the active surface, whereas a tensile stress represents attractive interactions and the microcantilever bends toward the functionalized side.

Key to the development and implementation of cantilever-based sensing and actuating technologies is the ability to precisely control the direction and amplitude of the cantilever movement. This level of control requires a comprehensive understanding of the origin of the surface stress generated in the (bio)chemical system under investigation. Nonetheless, the factors and phenomena contributing to both the nature (compressive/tensile) and magnitude of the surface stress in microcantilever experiments are often difficult to identify, especially

(7) Lavrik, N. V.; Sepaniak, M. J.; Datskos, P. G. *Rev. Sci. Instrum.* **2004**, *75*, 2229–2253.
(8) Goeders, K. M.; Colton, J. S.; Bottomley, L. A. *Chem. Rev.* **2008**, *108*, 522–542.
(9) Raiteri, R.; Grattarola, M.; Berger, R. *Mater. Today* **2002**, *5*, 22–29.
(10) Waggoner, P. S.; Craighead, H. G. *Lab Chip* **2007**, *7*, 1238–1255.
(11) Singamaneni, S.; LeMieux, M. C.; Lang, H. P.; Gerber, Ch.; Lam, Y.; Zauscher, S.; Datskos, P. G.; Lavrik, N. V.; Jiang, H.; Naik, R. R.; Bunning, T. J.; Tsukruk, V. V. *Adv. Mater.* **2008**, *20*, 653–680.
(12) Fritz, J.; Baller, M. K.; Lang, H. P.; Rothuizen, H.; Vettiger, P.; Meyer, E.; Güntherodt, H.-J.; Gerber, C.; Gimzewski, J. K. *Science* **2000**, *288*, 316–318.
(13) Fritz, J.; Cooper, E. B.; Gaudet, S.; Sorger, P. K.; Manalis, S. R. *Proc. Natl. Acad. Sci. U.S.A.* **2002**, *99*, 14142–14146.
(14) Mukhopadhyay, R.; Lorentzen, M.; Kjems, J.; Besenbacher, F. *Langmuir* **2005**, *21*, 8400–8408.
(15) Shu, W.; Liu, D.; Watari, M.; Riener, C. K.; Strunz, T.; Welland, M. E.; Balasubramanian, S.; McKendry, R. A. *J. Am. Chem. Soc.* **2005**, *127*, 17054–17060.
(16) McKendry, R. A.; Zhang, J.; Arntz, Y.; Strunz, T.; Hegner, M.; Lang, H. P.; Baller, M. K.; Certa, U.; Meyer, E.; Güntherodt, H.-J.; Gerber, C. *Proc. Natl. Acad. Sci. U.S.A.* **2002**, *99*, 9783–9788.
(17) Wu, G.; Ji, H.; Hansen, K.; Thundat, T.; Datar, R.; Cote, R.; Hagan, M. F.; Chakraborty, A. K.; Majumdar, A. *Proc. Natl. Acad. Sci. U.S.A.* **2001**, *98*, 1560–1564.
(18) Stachowiak, J. C.; Yue, M.; Castelino, K.; Chakraborty, A.; Majumdar, A. *Langmuir* **2006**, *22*, 263–268.
(19) Álvarez, M.; Carrascosa, L. G.; Moreno, M.; Calle, A.; Zaballos, Á.; Lechuga, L. M.; Martínez, A. C.; Tamayo, J. *Langmuir* **2004**, *20*, 9663–9668.
(20) Khaled, A.-R. A.; Vafia, K.; Yang, M.; Zhang, X.; Ozkan, C. S. *Sens. Actuators, B* **2003**, *94*, 103–115.
(21) Hagan, M. F.; Majumdar, A.; Chakraborty, A. K. *J. Phys. Chem. B* **2002**, *106*, 10163–10173.
(22) Yue, M.; Stachowiak, J. C.; Lin, H.; Datar, R.; Cote, R.; Majumdar, A. *Nano Lett.* **2008**, *8*, 520–524.
(23) Wu, G.; Datar, R. H.; Hansen, K. M.; Thundat, T.; Cote, R. J.; Majumdar, A. *Nat. Biotechnol.* **2001**, *19*, 856–860.
(24) Ndieyira, J. W.; Watari, M.; Barrera, A. D.; Zhou, D.; Vögtli, M.; Batchelor, M.; Cooper, M. A.; Strunz, T.; Horton, M. A.; Abell, C.; Rayment, T.; Aeppli, G.; McKendry, R. A. *Nat. Nanotechnol.* **2008**, *3*, 691–696.
(25) Backmann, N.; Zahnd, C.; Huber, F.; Bietsch, A.; Plückthun, A.; Lang, H.-P.; Güntherodt, H.-J.; Hegner, M.; Gerber, C. *Proc. Natl. Acad. Sci. U.S.A.* **2005**, *102*, 14587–14592.
(26) Savran, C. A.; Knudsen, S. M.; Ellington, A. D.; Manalis, S. R. *Anal. Chem.* **2004**, *76*, 3194–3198.
(27) Park, J.; Ryu, J.; Choi, S. K.; Seo, E.; Cha, J. M.; Ryu, S.; Kim, J.; Kim, B.; Lee, S. H. *Anal. Chem.* **2005**, *77*, 6571–6580.
(28) Ilic, B.; Yang, Y.; Craighead, H. G. *Appl. Phys. Lett.* **2004**, *85*, 2604–2606.
(29) Godin, M.; Williams, P. J.; Tabard-Cossa, V.; Laroche, O.; Beaulieu, L. Y.; Lennox, R. B.; Grütter, P. *Langmuir* **2004**, *20*, 7090–7096.
(30) Berger, R.; Delamarche, E.; Lang, H. P.; Gerber, C.; Gimzewski, J. K.; Meyer, E.; Güntherodt, H.-J. *Science* **1997**, *276*, 2021–2024.
(31) Berger, R.; Delamarche, E.; Lang, H. P.; Gerber, C.; Gimzewski, J. K.; Meyer, E.; Güntherodt, H.-J. *Appl. Phys. A: Mater. Sci. Process.* **1998**, *66*, S55–S59.
(32) Kohale, S.; Molina, S. M.; Weeks, B. L.; Khare, R.; Hope-Weeks, L. J. *Langmuir* **2007**, *23*, 1258–1263.
(33) Desikan, R.; Lee, I.; Thundat, T. *Ultramicroscopy* **2006**, *106*, 795–799.
(34) Desikan, R.; Armel, S.; Meyer, H. M., III; Thundat, T. *Nanotechnology* **2007**, *18*, 424028.
(35) Watari, M.; Galbraith, J.; Lang, H.-P.; Sousa, M.; Hegner, M.; Gerber, C.; Horton, M. A.; McKendry, R. A. *J. Am. Chem. Soc.* **2007**, *129*, 601–609.
(36) Ji, H.-F.; Hansen, K. M.; Hu, Z.; Thundat, T. *Sens. Actuators, B* **2001**, *72*, 233–238.
(37) Fritz, J.; Baller, M. K.; Lang, H. P.; Strunz, T.; Meyer, E.; Güntherodt, H.-J.; Delamarche, E.; Gerber, Ch.; Gimzewski, J. K. *Langmuir* **2000**, *16*, 9694–9696.
(38) Raiteri, R.; Butt, H.-J.; Grattarola, M. *Electrochim. Acta* **2000**, *46*, 157–163.
(39) Sushko, M. L.; Harding, J. H.; Shluger, A. L.; McKendry, R. A.; Watari, M. *Adv. Mater.* **2008**, *20*, 3848–3853.
(40) Ji, H.-F.; Zhang, Y.; Purushotham, V. V.; Kondu, S.; Ramachandran, B.; Thundat, T.; Haynie, D. T. *Analyst* **2005**, *130*, 1577–1579.
(41) Ji, H.-F.; Dabestani, R.; Brown, G. M.; Britt, P. F. *Chem. Commun.* **2000**, 457–458.
(42) Ji, H.-F.; Thundat, T. *Biosens. Bioelectron.* **2002**, *17*, 337–343.
(43) Ji, H.-F.; Thundat, T.; Debastani, R.; Brown, G. M.; Britt, P. F.; Bonnesen, P. V. *Anal. Chem.* **2001**, *73*, 1572–1576.
(44) Brunt, T. A.; Chabala, E. D.; Rayment, T.; O'Shea, S. J.; Welland, M. E. *J. Chem. Soc. Faraday Trans.* **1996**, *92*, 3807–3812.
(45) Brunt, T. A.; Rayment, T.; O'Shea, S. J.; Welland, M. E. *Langmuir* **1996**, *12*, 5942–5946.
(46) Haiss, W. *Rep. Prog. Phys.* **2001**, *64*, 591–648.
(47) Tian, F.; Pei, J. H.; Hedden, D. L.; Brown, G. M.; Thundat, T. *Ultramicroscopy* **2004**, *100*, 217–233.
(48) Ibach, H.; Bach, C. E.; Giesen, M.; Grossmann, A. *Surf. Sci.* **1997**, *375*, 107–119.
(49) Lahav, M.; Durkan, C.; Gabai, R.; Katz, E.; Willner, I.; Welland, M. E. *Angew. Chem., Int. Ed.* **2001**, *40*, 4095–4097.
(50) Tabard-Cossa, V.; Godin, M.; Grütter, P.; Burgess, I.; Lennox, R. B. *J. Phys. Chem. B* **2005**, *109*, 17531–17537.
(51) Bumbu, G.-G.; Kircher, G.; Wolkenhauer, M.; Berger, R.; Gutmann, J. S. *Macromol. Chem. Phys.* **2004**, *205*, 1713–1720.
(52) Bumbu, G.-G.; Wolkenhauer, M.; Kircher, G.; Gutmann, J. S.; Berger, R. *Langmuir* **2007**, *23*, 2203–2207.
(53) Zhou, F.; Shu, W.; Welland, M. E.; Huck, W. T. S. *J. Am. Chem. Soc.* **2006**, *128*, 5326–5327.
(54) Zhou, F.; Biesheuvel, P. M.; Choi, E.-Y.; Shu, W.; Poetes, R.; Steiner, U.; Huck, W. T. S. *Nano Lett.* **2008**, *8*, 725–730.
(55) Valiaev, A.; Abu-Lail, N. I.; Lim, D. W.; Chilkoti, A.; Zauscher, S. *Langmuir* **2007**, *23*, 339–344.
(56) Baller, M. K.; Fritz, J. In *Protein Microarray Technology*; Kambhampati, D., Ed.; Wiley-VCH Verlag GmBH & Co. KGaA: Weinheim, 2004; pp 195−213.
(57) Stoney, G. G. *Proc. R. Soc. London Ser. A.* **1909**, *82*, 172–175.
(58) Godin, M.; Tabard-Cossa, V.; Grütter, P. *Appl. Phys. Lett.* **2001**, *79*, 551–553.
(59) Tabard-Cossa, V.; Godin, M.; Beaulieu, L. Y.; Grütter, P. *Sens. Actuators, B* **2006**, *119*, 352–354.
(60) Tabard-Cossa, V.; Godin, M.; Beaulieu, L. Y.; Grütter, P. *Sens. Actuators, B* **2005**, *107*, 233–241.

those involving inherently complex biomolecular interactions. For example, DNA hybridization at oligonucleotide-modified cantilevers has received a lot of attention.[12,13,15−18] Steric and electrostatic repulsions, configuration entropy, hydration forces, conformational changes, and changes in osmotic pressure have all been proposed to contribute to the resulting surface stress. Furthermore, these contributions may compete with each other rendering nontrivial the interpretation of the surface stress arising from multiple interactions at the cantilever interface. This is supported by ongoing debates in the literature.[12,16,17,19−21,35]

Studies have also demonstrated that the selectivity and sensitivity of microcantilever systems rely heavily on the reproducible formation of a functional layer on one surface of the cantilever.[29,32,33,61−65] In this regard, chemically well-defined SAMs formed by ω-functionalized alkanethiols on noble metal surfaces can provide a model system with tailorable and reproducible interfacial chemistry, enabling one to probe specific molecular events. For example, investigations of the evolution of the surface stress during the chemisorption of *n*-alkanethiols onto gold-coated cantilevers have provided some much needed insight into the experimental factors and chemical interactions that drive the self-assembly process and determine the predominant structural phase adopted by the alkanethiolates.[29−34] Other work involving the pH titration of microcantilevers functionalized with carboxylic acid-terminated alkanethiolate SAMs has demonstrated that the in-plane surface forces which dictate the magnitude and nature of the surface stress associated with protonation/deprotonation reactions are sensitive to the solution pH, ionic strength, solution ion composition, as well as the alkyl chain length.[12,35,39] These findings with acidic SAMs are of broader relevance to understanding the molecular origins of surface stress at charged solid interfaces and in biological interactions. The studies cited above demonstrate that, in fact, micromechanical cantilevers can be very valuable tools for the investigation and characterization of SAMs.

In the study reported here, we used a ferrocenylundecanethiolate SAM on a gold-coated cantilever ($FcC_{11}SAu$) as a model system to investigate the origin of the surface stress generated by faradaic electrochemistry. We have extended a preliminary investigation[66] to (i) quantify the cantilever deflection/surface stress changes and (ii) probe the dynamics of the system. These investigations enable an assessment of the actuation properties of the ferrocenyl-modified surface and the identification of the molecular phenomena giving rise to the redox-induced deflection. Ferrocenylalkanethiolate SAMs are probably the most studied electroactive SAMs and the electrochemistry of single-component systems as well as of mixed monolayers consisting of ferrocenylalkanethiolates and inert alkanethiolates is extensively documented in the literature.[67−78] Ferrocene-terminated alkanethiolate SAMs exhibit relatively straightforward electrochemistry, meaning that every surface-tethered ferrocene can undergo a reversible one-electron redox reaction. Oxidation of the neutral ferrocene to the ferrocenium cation involves coupled electron-transfer and anion-pairing reactions.[67] Studies have also shown that the oxidation of the ferrocene to ferrocenium leads to changes in the water contact angle and a molecular reorientation.[69,70,76,79−84] These redox-induced changes in surface wettability and monolayer organization can drive macroscopic phenomena at ferrocenyl monolayer interfaces, such as the flow of aqueous solutions[80] and the orientation of liquid crystals,[85] and have been taken into account in our interpretation of the surface stress results. In our $FcC_{11}SAu$ microcantilever investigations, the environmental parameters remain unaltered (i.e., solvent, electrolyte concentration, temperature, and pH), and an electrical potential is used as an external stimulus to trigger specific molecular orientational changes by the electrochemical generation of ferrocenium. To determine the mechanism of the microcantilever response, the number and distribution of the immobilized ferrocenium cations were varied with time by linearly scanning the potential across the oxidation region or a specific number of ferroceniums was instantaneously created by the application of a fixed potential. The cantilever deflection of mixed $FcC_{11}S-/C_{11}SAu$ SAMs containing different populations of "clustered" vs "isolated" ferrocenes was also compared with that of pure $FcC_{11}SAu$ monolayers to determine the effect of ferrocenium alkanethiolate interactions on the surface stress.

Systems that are capable of converting electrical energy into mechanical motion are needed for a wide range of applications, e.g. robotics, artificial muscles, optical displays, and microfluidic devices. Conducting polymers have received a lot of attention as electroactuators, and the redox-induced deflection of polyanaline-[49] and polypyrrole-coated[50] cantilevers has been investigated. These conducting polymer-coated cantilever systems are only superficially akin to the $FcC_{11}SAu$ cantilevers used in the present study. The quantity of charge per area generated during oxidation of the polyaniline and polypyrrole multilayer

(61) Tabard-Cossa, V.; Godin, M.; Burgess, I. J.; Monga, T.; Lennox, R. B.; Grütter, P. *Anal. Chem.* **2007**, *79*, 8136–8143.
(62) Headrick, J. J.; Sepaniak, M. J.; Lavrik, N. V.; Datskos, P. G. *Ultramicroscopy* **2003**, *97*, 417–424.
(63) Lavrik, N. V.; Tipple, C. A.; Sepaniak, M. J.; Datskos, P. G. *Chem. Phys. Lett.* **2001**, *336*, 371–376.
(64) Hansen, A. G.; Mortensen, M. W.; Andersen, J. E. T.; Ulstrup, J.; Kühle, A.; Garnaes, J.; Boisen, A. *Probe Microsc.* **2001**, *2*, 139–150.
(65) Mertens, J.; Calleja, M.; Ramos, D.; Tarýn, A.; Tamayo, J. *J. Appl. Phys.* **2007**, *101*, 034904.
(66) Quist, F.; Tabard-Cossa, V.; Badia, A. *J. Phys. Chem. B* **2003**, *107*, 10691–10695.
(67) Finklea, H. O. In *Electroanalytical Chemistry*; Bard, A. J., Rubinstein, I., Eds.; Marcel Dekker: New York, 1996; Vol. 19, pp 109−335 and references therein.
(68) Weber, K. S.; Creager, S. E. *J. Electroanal. Chem.* **1998**, *458*, 17–22.
(69) Valincius, G.; Niaura, G.; Kazakevičienė, B.; Talaikytė, Z.; Kažemėkaitė, M.; Butkus, E.; Razumas, V. *Langmuir* **2004**, *20*, 6631–6638.
(70) Kazakevičienė, B.; Valincius, G.; Niaura, G.; Talaikytė, Z.; Kažemėkaitė, M.; Razumas, V.; Plaušinaitis, D.; Teišerskienė, A.; Lisauskas, V. *Langmuir* **2007**, *23*, 4965–4971.
(71) Ju, H.; Leech, D. *Phys. Chem. Chem. Phys.* **1999**, *1*, 1549–1554.
(72) Lee, L. Y. S.; Sutherland, T. C.; Rucareanu, S.; Lennox, R. B. *Langmuir* **2006**, *22*, 4438–4444.
(73) Sato, Y.; Mizutani, F.; Shimazu, K.; Ye, S.; Uosaki, K. *J. Electroanal. Chem.* **1999**, *474*, 94–99.
(74) Kondo, T.; Okamura, M.; Uosaki, K. *J. Organomet. Chem.* **2001**, *637−639*, 841–844.
(75) Auletta, T.; van Veggel, F. C. J. M.; Reinhoudt, D. N. *Langmuir* **2002**, *18*, 1288–1293.
(76) Kazakevičienė, B.; Valincius, G.; Niaura, G.; Talaikytė, Z.; Kažemėkaitė, M.; Razumas, V. *J. Phys. Chem. B* **2003**, *107*, 6661–6663.
(77) Viana, A. S.; Jones, A. H.; Abrantes, L. M.; Kalaji, M. *J. Electroanal. Chem.* **2001**, *500*, 290–298.
(78) Weber, K.; Hockett, L.; Creager, S. *J. Phys. Chem. B* **1997**, *101*, 8286–8291.
(79) Sondag-Huethorst, J. A. M.; Fokkink, L. G. J. *Langmuir* **1994**, *10*, 4380–4387.
(80) Abbott, N. L.; Whitesides, G. M. *Langmuir* **1994**, *10*, 1493–1497.
(81) Uosaki, K.; Sato, Y.; Kita, H. *Langmuir* **1991**, *7*, 1510–1514.
(82) Popenoe, D. D.; Deinhammer, R. S.; Porter, M. D. *Langmuir* **1992**, *8*, 2521–2530.
(83) Ye, S.; Sato, Y.; Uosaki, K. *Langmuir* **1997**, *13*, 3157–3161.
(84) Ye, S.; Haba, T.; Sato, Y.; Shimazu, K.; Uosaki, K. *Phys. Chem. Chem. Phys.* **1999**, *1*, 3653–3659.
(85) Luk, Y.-Y.; Abbott, N. L. *Science* **2003**, *301*, 623–626.

films is ca. 300[86,87] to 2000[88] times greater than that electrogenerated at the $FcC_{11}SAu$ cantilever. Moreover, in the macromolecular systems, stress changes result from the combined effects of physical swelling of the charged polymer matrix (due to the incorporation of counterions and solvent)[49,50] and the interaction of the supporting electrolyte ions with the underlying metal surface[50] (referred to as charge-induced surface stress) in areas where the polymer film does not properly adhere to the microcantilever as well as through defects in the polymer matrix. The contribution from charge-induced ion adsorption to the surface stress complicates the quantification of the redox-induced surface stress in conducting polymer actuators. By contrast, the stress changes in the SAM system are more straightforwardly attributable to redox-induced phenomena since solvent[73,81,89] and ion (perchlorate)[69,70,73,81,89] penetration into a full-coverage, close-packed $FcC_{11}SAu$ monolayer film is significantly inhibited.

Finally, it is important to note that a number of investigations employing gold-coated microcantilevers modified with functionalized SAMs have attributed the observed micromechanical deflection to *collective* in-plane molecular interactions.[12,16,17,90,91] For example, Stoddart and co-workers tethered to gold-coated microcantilevers linear molecular muscles based on bistable [3]rotaxanes consisting of a pair of mechanically mobile rings encircling a single dumbbell. The redox-controlled collective movement of the rings along the dumbbell induced a contractile strain on the surface of the microcantilever which caused it to bend.[90,91] The micromechanical motion arising from the hybridization of complementary oligonucleotides has also been attributed to collective phenomena within the biomolecular layer.[12,14−17] While these experiments claim collective interactions, there is limited evidence to support the mechanism of the microcantilever response. In the case of our $FcC_{11}SAu$ microcantilevers, electrochemistry provides an independent measure or count of the surface-activated species, thereby allowing us to establish that the microcantilever responds to collective molecular reorientations rather than to single electron transfer/anion pairing events. This finding has important consequences for employing SAM-functionalized cantilever microdevices for quantification in (bio)analytical chemistry.

Results and Discussion

Electrochemical Characterization of the $FcC_{11}SAu$ Microcantilevers. The cyclic voltammograms (CVs) obtained for the oxidation/reduction in 0.10 M $NaClO_4$/0.01 M $HClO_4$ of $FcC_{11}SAu$ monolayers formed on the AFM microcantilevers (Figure S1, Supporting Information) resemble those previously published for 100% $FcC_{11}SAu$[81,83,92] and $FcC_{12}SAu$[66,72] SAMs on macroscopic polycrystalline Au electrodes, and will be only briefly described here. Ferrocene oxidation and ferrocenium reduction peaks are observed at 0.39 and 0.38 V (vs Ag/AgCl), respectively. Shoulders are also present on the negative potential side of the main redox peaks. The presence of multiple voltammetric waves is attributable to the existence of electrochemically distinct ferrocene microenvironments.[72,75,93−95] The ferrocene surface coverage of 4.7 ($\pm$0.3) $\times$ 10^{-10} mol cm^{-2} ($Q_{Fc}{}^{+}$= 45 ($\pm$3) μC cm^{-2}), determined experimentally on macroscopic Au-coated slides prepared and functionalized in the same manner as the microcantilevers (see Supporting Information), is close to the theoretical value (4.5 $\times$ 10^{-10} mol cm^{-2}) expected from the close packing of ferrocene spheres of 6.6 Å diameter.[96]

Surface Stress Measurements. For the electrochemical microcantilever experiments presented in this paper, the measured electrochemical current arises mainly from the chip substrate, given the relative $FcC_{11}SAu$-covered surface areas of the cantilevers, ~10^{-5}−10^{-4} cm^2, and chip, ~0.02−0.03 cm^2, immersed in the electrolyte solution. However, the measured PSD signal is associated with the free end of the V- or rectangular-shaped microcantilever, as verified below. A previous ToF-SIMS analysis of the $FcC_{12}SAu$-coated side of AFM probes revealed a homogeneous distribution of the ferrocene across the microcantilever and chip surfaces.[66] We can therefore correlate the microcantilever deflection with the electrochemistry data collected.

Shown in Figure 1 are the typical current (Figure 1A) and deflection (Figure 1B) responses obtained for successive CV scans of a $FcC_{11}SAu$-coated microcantilever in perchlorate solution. The PSD output voltage was converted to a cantilever beam deflection, Δz (Figure 1B, left *y*-axis), which was then used to calculate the difference in surface stress, $\Delta\sigma$ (Figure 1B, right *y*-axis), between the $FcC_{11}SAu$-modified and unmodified (silicon/silicon oxide or silicon nitride) sides of the microcantilever, as outlined in the Experimental Section (Supporting Information). In this work, microcantilever deflections that result in a positive increase in the PSD voltage indicate a bending of the cantilever away from the gold-coated face because of compressive surface stress, which we express as a negative value, in accordance with common sign convention.[97]

A number of control experiments were initially completed to ensure that the microcantilever deflection and associated surface stress change arise *primarily* from the ferrocene/ferrocenium redox reaction. To start, the corresponding PSD signals measured at the apex of the microcantilever beam vs a region of the support chip during potential cycling are presented in Figure S2, Supporting Information. As expected, no significant change in the PSD voltage is observed when the laser is focused on the immobile chip. We can therefore affirm that the PSD response tracks the deflection of the mobile and flexible microcantilever and rule out a contribution from potential-induced changes in the reflectivity of the monolayer-coated gold surface.[98−100] The microcantilever is deflected to a higher PSD

(86) The quantity of charge per cm^2 was estimated using the polyaniline film thickness of 190 nm reported by Lahav et al. (see ref 49) and the relation between the anodic charge density and the electropolymerized film thickness (see ref 87, eq 3).
(87) Guiseppi-Elie, A.; Pradhan, S. R. *Chem. Mater.* **1993**, *5*, 1474–1480.
(88) The charge per area was estimated from the reported polypyrrole film thicknesses (t (nm)) using the equation t (nm) = 2.8Q (mC cm^{-2}) given in ref 50.
(89) Shimazu, K.; Yagi, I.; Sato, Y.; Uosaki, K. *J. Electroanal. Chem.* **1994**, *372*, 117–124.
(90) Huang, T. J.; Brough, B.; Ho, C.-M.; Liu, Y.; Flood, A. H.; Bonvallet, P. A.; Tseng, H.-R.; Stoddart, J. F.; Baller, M.; Magonov, S. *Appl. Phys. Lett.* **2004**, *85*, 5391–5393.
(91) Liu, Y.; Flood, A. H.; Bonvallet, P. A.; Vignon, S. A.; Northrop, B. H.; Tseng, H.-R.; Jeppesen, J. O.; Huang, T. J.; Brough, B.; Baller, M.; Magonov, S.; Solares, S. D.; Goddard, W. A.; Ho, C.-M.; Stoddart, J. F. *J. Am. Chem. Soc.* **2005**, *127*, 9745–9759.
(92) Ohtsuka, T.; Sato, Y.; Uosaki, K. *Langmuir* **1994**, *10*, 3658–3662.
(93) Fujii, S.; Kurokawa, S.; Murase, K.; Lee, K.-H.; Sakai, A.; Sugimura, H. *Electrochim. Acta* **2007**, *52*, 4436–4442.
(94) Calvente, J. J.; Andreu, R.; Molero, M.; Lopez-Perez, G.; Domínguez, M. *J. Phys. Chem. B* **2001**, *105*, 9557–9568.
(95) Smith, C. P.; White, H. S. *Anal. Chem.* **1992**, *64*, 2398–2405.
(96) Chidsey, C. E. D.; Bertozzi, C. R.; Putvinski, T. M.; Mujsce, A. M. *J. Am. Chem. Soc.* **1990**, *112*, 4301–4306.
(97) Ibach, H. *Surf. Sci. Rep.* **1997**, *29*, 195–263.
(98) Badia, A.; Arnold, S.; Scheumann, V.; Zizlsperger, M.; Mack, J.; Jung, G.; Knoll, W. *Sens. Actuators, B* **1999**, *54*, 145–165.

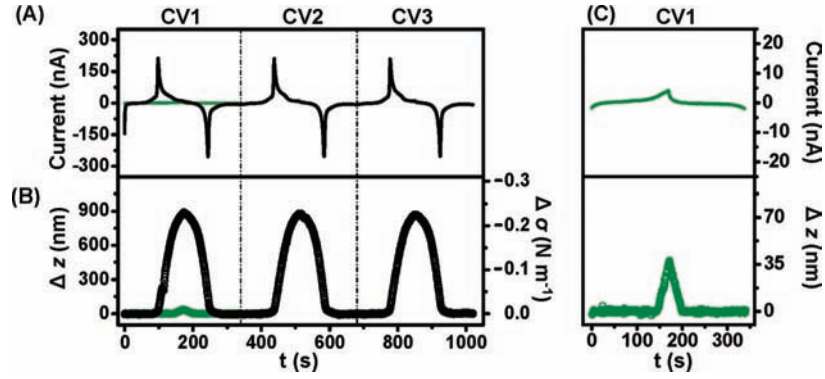

Figure 1. (A) Typical CV traces of $FcC_{11}SAu$ (black line) and $C_{11}SAu$ (green line) modified microcantilever substrates in 0.1 M $NaClO_4$/0.01 M $HClO_4$. The potential scan rate was 5 mV s^{-1}. (B) Corresponding deflection (Δz, left axis) and surface stress ($\Delta\sigma$, right axis) profiles for the $FcC_{11}SAu$ (black circle) and $C_{11}SAu$ (green circle) modified V-shaped microcantilevers ($k = 0.011 \pm 0.002$ N m^{-1}) in 0.1 M $NaClO_4$/0.01 M $HClO_4$. (C) Zoom-in of the current−time (top) and deflection-time (bottom) traces recorded by cyclic voltammetry for the $C_{11}SAu$ microcantilever.

voltage upon oxidation of the ferrocene (neutral form) to ferrocenium (cationic form) and returns to nearly its initial position when the ferrocenium is reduced back to ferrocene, although a continuous drift in either the positive or negative direction is usually observed with time. Single microcantilever experiments in solution are susceptible to spurious deflections that may be caused by temperature fluctuations, the release of stress accumulated during the gold evaporation process or the slow rearrangement of the molecules in the SAM.[56] This background drift can be easily corrected for mathematically and does not affect the magnitude of the maximum deflection observed in a given oxidation/reduction cycle (Figure S3, Supporting Information).

Next, inert $C_{11}SAu$-coated cantilevers were used as nonferrocenylated analogues to verify that the potential-induced deflection of the $FcC_{11}SAu$-modified cantilevers reported herein is not dominated by charge-induced ion adsorption to the underlying gold surface. Such verification is pertinent because investigations of the potential-induced surface stress response of organic (ultra)thin film-modified metal-coated microcantilevers have reported deflections resulting from ion penetration and adsorption to the metal surface.[50] In the absence of free redox species in solution, SAMs of *n*-alkanethiols of chain length $\geq$10 carbons are relatively impermeable to various electrolyte ions in aqueous medium within the potential range of $\sim$−0.2 V to $\sim$+0.5 V (vs Ag/AgCl), provided that the monolayers are sufficiently defect-free.[101] In the present investigation, monolayer capacitances of 1.4 ($\pm$0.1) μF cm^{-2} and 1.8 ($\pm$0.2) μF cm^{-2}, were found for the $C_{11}SAu$ and $FcC_{11}SAu$ SAMs, respectively, in perchlorate solution.[102] These results are in good agreement with previously reported capacitances of 1.5 μF cm^{-2} for $C_{11}SAu$[103] and 1.5 to 2.0 μF cm^{-2} for $FcC_{11}SAu$[104] and $FcCO_2C_{11}SAu$[79] SAMs. Even though the molecular packing density of the $FcC_{11}SAu$ SAM (2.5 molecules nm^{-2}) is $\sim$0.6 × that of the $C_{11}SAu$ SAM (4.7 molecules nm^{-2})[105] due to the bulky terminal ferrocene, their capacitances are comparable. The $C_{11}SAu$ system should therefore provide a reasonable estimate of the contribution of ion permeation to the surface stress. As expected, no faradaic current was observed (Figure 1C, top panel) upon cycling the potential of a $C_{11}SAu$ microcantilever from −0.10 to +0.75 V (vs Ag/AgCl) in 0.10 M $NaClO_4$/0.01 M $HClO_4$ solution. A deflection of the microcantilever was however detected (Figure 1C, bottom panel) at potentials >+0.60 V. The magnitude of the resulting surface stress change is $\sim$−0.01 N m^{-1}, which corresponds to $\sim$5% of the response observed for the $FcC_{11}SAu$ microcantilever over the same potential scan range (Figure 1B). We therefore attribute the potential-induced deflection/surface stress change of a $FcC_{11}SAu$ microcantilever principally to the oxidation/reduction of the surface-bound ferrocene/ferrocenium species.

The data obtained for 43 different $FcC_{11}SAu$-modified probe chips shows that the SAM and magnitude of the cantilever deflection are stable over three successive redox cycles run at a potential scan rate of 5 mV/s between −0.10 to +0.75 V in 0.10 M $NaClO_4$/0.01 M $HClO_4$ solution (Figure 1). Between the first and third CV scan, there is an average variation of 1% in Q_{Fc}^{+} and a change of 7% in the peak deflection amplitude, although 20% of the microcantilevers exhibited a peak amplitude change of $\leq$2%.

A systematic investigation of the effect of the microcantilever spring constant (k) on the measured deflection and surface stress change was undertaken. Such an effect has not usually been investigated in microcantilever experiments, but can be important to understanding the magnitude of the observed stress.[23] Figure 2 summarizes the results obtained for $FcC_{11}Au$-modified microcantilevers ranging from a low k of 0.011 ($\pm$0.002) N m^{-1} to a considerably stiffer k of 0.791 ($\pm$0.004) N m^{-1}. The values reported are the maximum deflections measured at the switching potential of +0.75 V, where all of the ferrocene has been oxidized to ferrocenium. As expected, the largest Δz was recorded for the floppiest microcantilever (k = 0.01 N m^{-1}) and the magnitude of the deflection decreases pseudoexponentially from $\sim$0.8 μm to $\sim$60 nm as k increases from $\sim$0.01 to $\sim$0.8 N m^{-1} (Figure 2A). The $\Delta\sigma$ values calculated from the microcantilever deflections are however very similar, i.e. −0.17 to −0.23 N m^{-1}, for k's ranging between $\sim$0.01 to $\sim$0.13 N

(99) Heaton, R. J.; Peterson, A. W.; Georgiadis, R. M. *Proc. Natl. Acad. Sci. U.S.A.* **2001**, *98*, 3701–3704.
(100) Norman, L. L.; Badia, A. *Langmuir* **2007**, *23*, 10198–10208.
(101) Boubour, E.; Lennox, R. B. *J. Phys. Chem. B* **2000**, *104*, 9004–9010.
(102) The capacitance was measured by CV on macroscopic gold film electrodes in perchlorate solution at−0.050 V (potential at which there is no ferrocene oxidation). The potential range of−0.150 V to +0.050 V (vs Ag/AgCl) was scanned at a rate of 100 mV s^{-1}.
(103) Porter, M. D.; Bright, T. B.; Allara, D. L.; Chidsey, C. E. D. *J. Am. Chem. Soc.* **1987**, *109*, 3559–3568.
(104) Cruañes, M. T.; Drickamer, H. G.; Faulkner, L. R. *Langmuir* **1995**, *11*, 4089–4097.
(105) Sigal, G. B.; Mrksich, M.; Whitesides, G. M. *J. Am. Chem. Soc.* **1998**, *120*, 3464–3473.

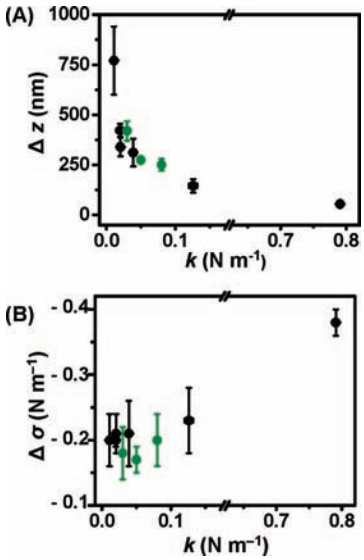

Figure 2. Plots of the (A) microcantilever deflection (Δz) and (B) microcantilever surface stress ($\Delta\sigma$) vs the spring constant (k) for $FcC_{11}SAu$ modified microcantilevers. In both graphs solid black dots represent SiN_x microcantilevers while the solid green dots represent Si/SiO_x microcantilever measurements. The Δz values reported for each spring constant are the average and standard error measured for at least four different cantilevers of that spring constant. The Si/SiO_x (solid green dots) cantilevers are all rectangular in shape, whereas the SiN_x (solid black dots) microcantilevers are V-shaped, except for the cantilever with $k = 0.0206$ (± 0.0004) N m^{-1}.

m^{-1} (Figure 2B). This range encompasses the microcantilever spring constants typically employed in microcantilever experiments. Furthermore, the $\Delta\sigma$ measured for the electrochemical oxidation/reduction of $FcC_{11}SAu$ SAMs does not depend on the characteristics of the microcantilever, such as shape (triangular or rectangular) or material (silicon/silicon oxide or silicon nitride), as shown in Figure 2.

Microcantilever Deflection vs Quantity of Electrogenerated Ferrocenium. To rationalize the electrochemically induced deflection of the $FcC_{11}SAu$-modified microcantilever, we compare the % microcantilever deflection−potential profile with that of the fractional coverage of ferrocenium (Φ_{Fc}^+) electrogenerated at potential scan rates of 10, 5, and 1 mV s^{-1} (Figure 3). The following significant observations can be made from such a comparison. First, both curves exhibit a sigmoidal shape. The % change in microcantilever deflection (%Δz) attains a limiting value (defined as 100%) when all of the ferrocene has been converted to ferrocenium in the anodic scan (i.e., $\Phi_{Fc}^+ = 1$), and a constant value of 0% as Φ_{Fc}^+ approaches 0 in the cathodic scan. This observation is consistent with the $FcC_{11}SAu$ microcantilever deflection resulting principally from a redox transformation of the ferrocenyl group. Interestingly, bending of the microcantilever is detectable only after ∼15−20% conversion of the ferrocene to ferrocenium, i.e., $\Phi_{Fc}^+ \approx 0.2$ (at the usual scan rate of 5 mV s^{-1}). In other words, the microcantilever deflection is triggered by the electrogeneration of $\sim 5.8 \times 10^{13}$ Fc^+s per cm^2 ($\Phi_{Fc}^+ \approx 0.2$). On the reverse scan, the microcantilever has already returned to within 15−30% of its original resting position after 50% of the ferrocenium is reduced back to ferrocene ($\Phi_{Fc}^+ \approx 0.5$). The appreciable offset of the microcantilever deflection−potential response from the Φ_{Fc}^+ (i.e., integrated current)−potential curve could not be diminished by using a more flexible microcantilever (0.01 N m^{-1} vs 0.10 N m^{-1}) or a slower potential scan rate (1 mV s^{-1} vs 10 mV s^{-1}).

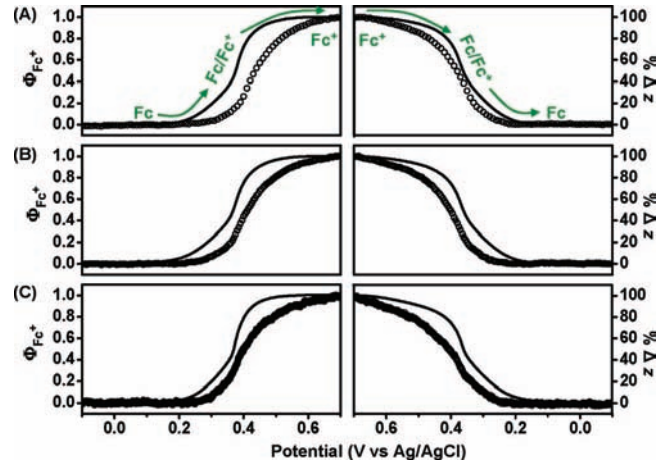

Figure 3. Plots of the fractional coverage (Φ_{Fc}^+) of ferrocenium (—) and % change in cantilever deflection (%Δz, ○) vs the applied potential for scan rates: (A) 10 mV s^{-1}, (B) 5 mV s^{-1}, and (C) 1 mV s^{-1}. The left panel of the graphs represent the anodic scan (−0.10 to +0.70 V), whereas the right panel represents the cathodic scan (+0.70 to −0.10 V). Φ_{Fc}^+ was determined by integrating incrementally the areas under the anodic and cathodic current−potential curves of the CVs after correcting for the charging current by a baseline approximation. The % change in the cantilever deflection was calculated by assigning the PSD signals at 0 V and +0.70 V to, respectively, the zero and maximum cantilever positions. The arrows indicate the direction of potential cycling for the redox cycle.

Φ_{Fc}^+ is directly related to electron transfer across the SAM−electrode interface. On the other hand, the cantilever deflection may arise from the accumulation of charge on the cantilever surface, causing there to be a time delay between the deflection and current responses. To investigate the cause of this offset, potential step-hold experiments were performed, where the applied potential was stepped from open circuit to potentials corresponding to $\Phi_{Fc}^+ = 0$ (0.050 V), 0.34 (0.340 V), 0.64 (0.385 V), 0.82 (0.415 V), and 0.99 (0.550 V). The potential holds were kept within the potential range where no deflection of the $C_{11}SAu$ microcantilever was observed (Figure 1C). The $\Delta\sigma$−time profiles (Figure 4A) demonstrate that the maximum $FcC_{11}SAu$ microcantilever deflections are obtained within ∼3 s of the potential step (i.e., 3 × microcantilever sampling time) and the deflections remain relatively constant during the potential hold interval of 50 s. A decrease of ∼10% was observed in the case of $\Phi_{Fc}^+ = 0.99$, probably because of some decomposition of the ferrocenium cations with time at the higher oxidizing potential (0.550 V).[82,106] The microcantilevers returned to their original positions within ∼3 s of the applied potential being stepped back to open circuit. The potential step-hold experiments indicate that the offset between the deflection−potential and integrated current−potential curves obtained in the CV experiments (Figure 3) is not due to the microcantilever having a longer response time due to charge accumulation. This is certainly true for the 1 mV s^{-1} cycles (slowest scan rate used), in which the applied potential changes by only ∼3 mV within the ∼3 s that it takes the microcantilever to reach its steady-state position at each point of the potential scan. More importantly, the $\Delta\sigma$ values obtained at different Φ_{Fc}^+ values for ferrocene oxidation by CV are very close to those acquired in the potential step and hold experiments (Figure 4B). This observation supports the notion that the deflections recorded

(106) Green, J.-B. D.; McDermott, M. T.; Porter, M. D. *J. Phys. Chem.* **1996**, *100*, 13342–13345.

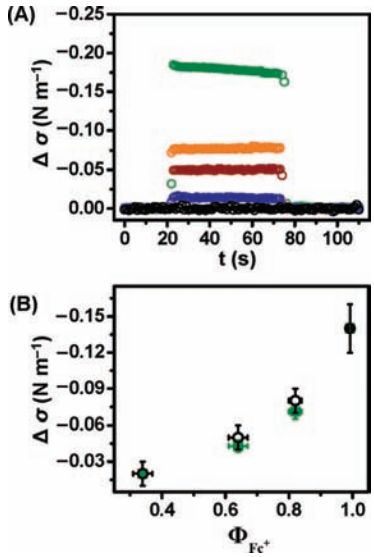

Figure 4. (A) Time-dependent surface stress profiles observed for a $FcC_{11}SAu$ microcantilever ($k = 0.024 \pm 0.002$ N m^{-1}) in single-step potential-hold experiments, where the potential was stepped from open circuit potential to potentials corresponding to ferrocenium surface coverages: $\Phi_{Fc}^{+} = 0$ (0.050 V, black), 0.34 (0.340 V, blue), 0.64 (0.385 V, red), 0.82 (0.415 V, orange), and 0.99 (0.550 V, green). (B) Plot of the $\Delta\sigma$ values obtained by potential step-hold (black circle) and cyclic voltammetry (green square) for a given Φ_{Fc}^{+}. The CVs were acquired at a scan rate of 5 mV s^{-1}.

during CV scans are not limited by the microcantilever response time but by collective events occurring at the microcantilever interface.

We propose that the delayed bending response of the $FcC_{11}SAu$ microcantilever under an applied potential is due to the measured current reporting individual redox events, whereas the microcantilever beam deflection reflects an ensemble of in-plane molecular interactions. Collective interactions are possible if there is a sufficient number of neighboring ferroceniums. Interactions between ferroceniums (vs isolated noninteracting ferroceniums) are detected electrochemically in binary SAMs when the surface mole fraction of ferrocene is ≥ 0.2, due to the presence of domains or clusters of ferrocene alkanethiolates.[72,75] In single-component FcRSAu, the oxidation of a ferrocene next to an already oxidized ferrocenium cation is unfavorable because of electrostatic or Coulombic repulsion between the charged moieties, so that a critical number of electrogenerated ferroceniums may be needed for neighboring interactions.[94,95] A simulation of the ferrocenium distribution as a function of Φ_{Fc}^{+} provides an approximate idea of the extent of neighboring ferrocenium interactions with the applied potential (Figure 5A), which we have used to rationalize the % deflection vs Φ_{Fc}^{+} behavior obtained experimentally (Figure 5B). Our crude modeling exercise consisted of placing ferroceniums in single fashion at random in a 36 × 36 grid (1296 molecules) and, for a given Φ_{Fc}^{+}, counting the number of ferroceniums which have more than one nearest neighbor.[107−110] A more accurate model

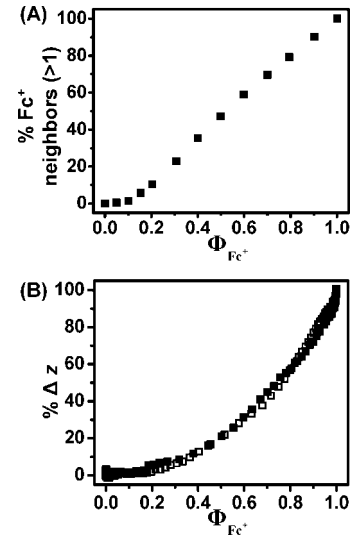

Figure 5. (A) A plot of the simulated ferrocenium nearest neighbor (>1) distribution vs the ferrocenium coverage (Φ_{Fc}^{+}) for a 36 × 36 grid (1296 molecules). (B) Plot of the % change in the cantilever deflection vs the fractional coverage of ferrocenium (Φ_{Fc}^{+}) for the anodic (■) and cathodic (□) scans.

would account for the actual ferrocene domain size (unknown parameter), loose hexagonal lattice structure,[111] and the number of nearest and next-nearest ferrocenium neighbors for a given Φ_{Fc}^{+}. Such an exercise is outside the scope of our modeling capabilities. The results of our simplified simulation (Figure 5A) are nevertheless informative as these reveal that the number of electrogenerated ferroceniums that are surrounded by more than one neighboring ferrocenium becomes significant starting at $\Phi_{Fc}^{+} \approx 0.15-0.20$, and the number increases nonlinearly as Φ_{Fc}^{+} increases. This calculated Φ_{Fc}^{+} onset is consistent with the minimum surface concentration required for electrochemically interacting ferrocenes in mixed SAMs.[72,75,94] More importantly, it coincides with the experimentally observed Φ_{Fc}^{+} range in which the onset of microcantilever deflection occurs (Figure 5B), suggesting that there is a correlation between the extent of the microcantilever deflection or bending and the number of neighboring ferroceniums.

Influence of the Ferrocene Surface Coverage on the Surface Stress Response. To verify our hypothesis that the observed microcantilever deflection arises from combined lateral interactions between ferrocenium-bearing alkylthiolates, we investigated mixed SAM-modified microcantilevers in which the electroactive ferrocenes are isolated from one another by an inert *n*-alkylthiolate matrix. The voltammetric parameters are of interest here as we investigate the consequence of the phase state ("isolated" vs "clustered") of the surface-confined ferrocenes on the microcantilever response. Typical CVs and corresponding $\Delta\sigma$ responses obtained for microcantilevers modified with binary $FcC_{11}S-/C_{11}SAu$ SAMs for which the $FcC_{11}S-$ concentration corresponds to ~35% and ~14% of the surface coverage (Γ_{Fc}) of a single-component $FcC_{11}SAu$ SAM (4.7 (±0.3) × 10^{-10} mol cm^{-2}) are depicted in Figure 6. The different surface concentrations were obtained by varying the

(107) Alkylthiol domain sizes typically range from 10 to 100 nm and contain between 350 to 38 000 alkylthiol molecules (see refs 108 and 109). For ferrocenylundecanethiol assembled on gold, the same size domains would contain 225 to 22 500 molecules. A Monte Carlo simulation showed that a 224-molecule system size is large enough to produce well-differentiated domains (see ref 110).

(108) Nelles, G.; Schönherr, H.; Jaschke, M.; Wolf, H.; Schaub, M.; Küther, J.; Tremel, W.; Bamberg, E.; Ringsdorf, H.; Butt, H.-J. *Langmuir* **1998**, *14*, 808–815.

(109) Fenter, P.; Eisenberger, P.; Liang, K. S. *Phys. Rev. Lett.* **1993**, *70*, 2447–2450.

(110) Siepmann, J. I.; McDonald, I. R. *Langmuir* **1993**, *9*, 2351–2355.

(111) Müller-Meskamp, L.; Lüssem, B.; Karthäuser, S.; Prikhodovski, S.; Homberger, M.; Simon, U.; Waser, R. *Phys. Stat. Sol. (A)* **2006**, *203*, 1448–1452.

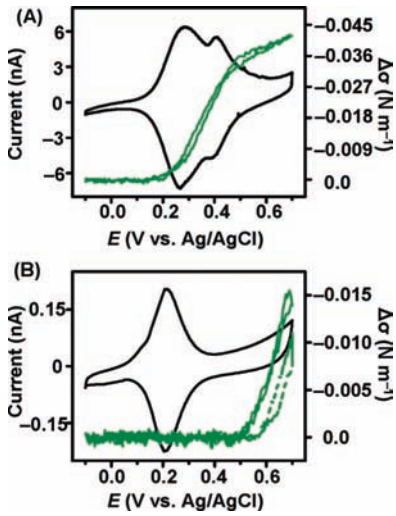

Figure 6. Typical CV traces (left axis, black line) and corresponding $\Delta\sigma$ responses (right axis, green line) obtained for microcantilevers modified with binary $FcC_{11}S-/C_{11}SAu$ SAMs for which the $FcC_{11}S-$ concentration is (A) ~35% and (B) ~14% of that of single-component $FcC_{11}SAu$ modified microcantilever substrates. The green dashed line in B is the stress response obtained for the $C_{11}SAu$ microcantilever shown in Figure 1C.

relative concentrations of $FcC_{11}SH$ and $C_{11}SH$ in the incubation solution. The resulting phase state of the mixed SAM depends on the relative concentrations and solubilities of the two thiols in the incubation solution.[72,112] The two-peak nature of the CV for $\Gamma_{Fc} \approx 35\%$ (Figure 6A) is consistent with a phase-separated monolayer where the $FcC_{11}S-$ are either isolated from one another (peak I, $E_{1/2} = 0.30 \pm 0.03$ V) or clustered together inside domains (peak II, $E_{1/2} = 0.41 \pm 0.01$ V).[72,75] A positive shift in $E_{1/2}$ for the clustered domains (peak II) results because electrostatic repulsion between ferrocenium cations renders the oxidation of neighboring ferrocenes less favorable,[72,75] as already mentioned. Using a redox peak deconvolution method described elsewhere,[72] the relative surface proportions of the isolated and clustered ferrocene species were estimated (Figure S4, Supporting Information). Briefly, peak I was fit to a Gaussian distribution and peak II was fit to a Lorentzian function.[113] Both peaks were fit using three free fitting parameters: peak position, peak width, and peak area. The deconvolution of the CVs obtained for the binary $FcC_{11}S-/C_{11}SAu$ ($\Gamma_{Fc} \approx 35\%$) substrates reveals that the "isolated" ferrocene moieties constitute ~62% (1.01×10^{-10} mol cm^{-2}) of the total surface-confined ferrocene, whereas ~38% (6.18×10^{-11} mol cm^{-2}) of the ferrocenes are found within close proximity to each other. For the $\Gamma_{Fc} \approx 14\%$ SAM (Figure 6B), the single symmetrical redox peak observed indicates that the $FcC_{11}SAu$ molecules are predominantly dispersed throughout the inert $C_{11}SAu$ matrix.[72,75] We expect that "isolated" ferrocenium moieties, which are not surrounded by other ferrocenium neighbors, but by inert $C_{11}S-$, will not contribute to the measured $\Delta\sigma$. Consistent with this hypothesis, the surface stress response of the 14% $FcC_{11}S-/C_{11}SAu$ SAM, -0.011 ± 0.007 N m^{-1}, is of essentially the same magnitude (within experimental variability) as the inert $C_{11}SAu$ SAM (Figure 6B). On the other hand, "clustered" ferroceniums experience environmental and steric constraints that cause the monolayer reorganization giving rise to the microcantilever deflection (vide infra). The size and shape of the domains formed by the aggregated $FcC_{11}S-$ are unknown, so that the observed $\Delta\sigma$ of -0.037 ± 0.006 N m^{-1} for the 35% $FcC_{11}S-/C_{11}SAu$ SAM cantilevers is a weighted average of all the in-plane interactions for a range of cluster sizes. The aggregated $FcC_{11}S-$ population comprising this binary SAM was determined to be 6.18×10^{-11} mol cm^{-2}, which corresponds to ~14% of the surface coverage of a full-coverage single-component analogue. The $\Delta\sigma$ measured for the 35% $FcC_{11}S-/C_{11}SAu$ cantilevers is ~18% of that observed for the single-component $FcC_{11}SAu$ ($\Delta\sigma = -0.20 \pm 0.04$ N m^{-1}). This proportional decrease in $\Delta\sigma$ is consistent with the microcantilever response arising from lateral interactions between aggregated ferroceniums.

Origin of the Redox-Induced Surface Stress Change. The measured $\Delta\sigma$ of -0.20 ± 0.04 N m^{-1} indicates that the electrochemical oxidation of the $FcC_{11}SAu$ SAM generates an average in-plane repulsive force of 132 pN per $Fc^+C_{11}S-$ molecule (calculated using a ferrocene diameter of 0.66 nm) and an internal film pressure of ca. 0.1 GPa ($= \Delta\sigma \times d^{-1}$,[30] where the thickness, d, of the $FcC_{11}SAu$ monolayer is 1.8 nm[100]). What are the repulsive lateral interactions that could generate such a force and cause the $Fc^+C_{11}SAu$ microcantilever to bend? To answer this question, we have considered the ion pair formation,[89,114−116] changes in interfacial properties,[79,80,106] and the molecular reorientation[69,70,77,82−84] that have been identified by various in situ electrochemical surface analytical methods to accompany electron transfer. Both contact angle[79,80] and AFM-adhesion force[106] measurements have reported that the oxidation of the surface-confined ferrocene adjacent to a polar carboxylate ($FcCO_2C_{11}SAu$) or carbonyl ($FcCOC_{15}SAu$) group results in a notably more hydrophilic interface. We also found a decrease in the static perchlorate solution contact angle, from 77 (±5)° to 65 (±4)°, upon oxidation of the terminal ferrocene to ferrocenium for the $FcC_{11}SAu$ SAM. This increased hydrophilicity results in a decrease in the interfacial (monolayer/water) surface tension so that one would intuitively expect to observe a *tensile* surface stress, corresponding to bending of the microcantilever toward the film-coated Au side, upon oxidation of the ferrocene to ferrocenium in aqueous perchlorate solution. Although a redox-induced change in the macroscopic wettability of the $FcC_{11}SAu$ surface may contribute to the overall surface stress measured, it clearly is not the source of the net *compressive* stress reported herein.

CV[96,115,116] and electrochemical quartz crystal microbalance[84,89] experiments have established that the hydrophobic perchlorate anions complex strongly with the terminal ferrocenium cations to form 1:1 ion pairs at the monolayer/solution interface. Ion pairing with a perchlorate anion facilitates the oxidation of the ferrocene by stabilizing the ferrocenium cation. This 1:1 ion pair formation should reduce the Coulombic repulsion between neighboring ferroceniums as well as between the positively charged Au surface and the terminal ferrocenium cations by the neutralization of the excess positive charge on the ferroceniums. Therefore, it is unlikely that repulsive Coulombic forces cause significant bending of the microcantilever.[117] Repulsive dipolar interactions between ferrocenium-bearing alkanethiolates ($Au^{\delta+}-S^{\delta-}-R^{\delta+}-Fc^+-ClO_4^-$) are expected to be even weaker.[118−120] The relative magnitudes of the adhesion forces between neutral

(112) Bain, C. D.; Evall, J.; Whitesides, G. M. *J. Am. Chem. Soc.* **1989**, *111*, 7155–7164.
(113) OriginPro 7.5 ed.; OriginLab Corporation.
(114) Chidsey, C. D. E. *Science* **1991**, *251*, 919–922.
(115) Creager, S. E.; Rowe, G. K. *Anal. Chim. Acta* **1991**, *246*, 233–239.
(116) Rowe, G. K.; Creager, S. E. *Langmuir* **1991**, *7*, 2307–2312.
(117) The average Coulombic force contribution of each individual ferrocenium−ferrocenium interaction (for unpaired ferroceniums) to the deflection of the cantilever, calculated using Coulomb's law, is only ~3 pN (for an **x**-vector along the length of the cantilever).

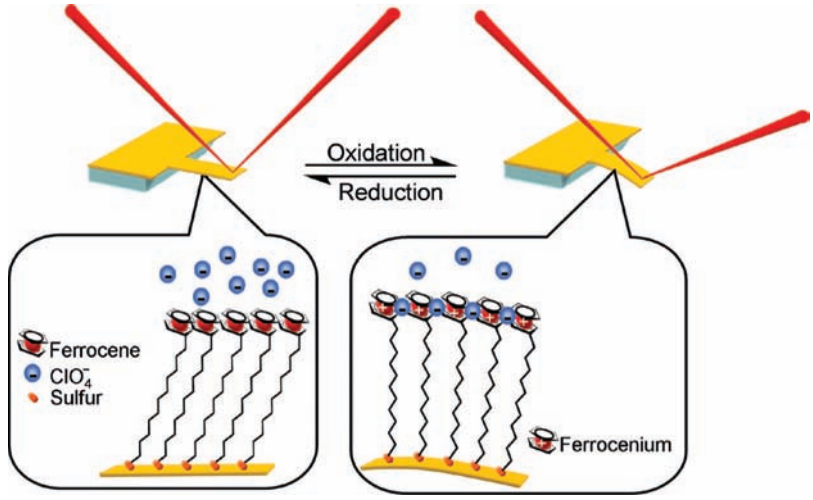

Figure 7. Schematic representation of the redox-induced deflection of $FcC_{11}SAu$ microcantilevers in perchlorate solution.

and oxidized polyvinylferrocene films in aqueous perchlorate solution have been measured by Hudson and Abruña.[121] No comparison can however be made between these adhesion force measurements and our surface stress measurements with regards to $Fc^+-ClO_4^-$ ion pair interactions since (i) AFM force spectroscopy probes *out-of-plane* adhesive forces between two surfaces in contact,[106] whereas the microcantilever measurements reflect *in-plane* forces acting at an interface and (ii) adhesion forces measured in liquid reflect the surface free energies of solvated functional groups rather than bare molecular interactions.[122]

A high-pressure electrochemical investigation of $FcC_{11}SAu$ SAMs by Cruañes et al. suggests that the complexation of the perchlorate to the ferrocenium requires a reorganization of the monolayer because of steric constraints.[104] CVs run at hydrostatic pressures ranging from 1 atm (ambient pressure) to 6000 atm show that the oxidation of the monolayer-confined ferrocene is thermodynamically and kinetically more difficult at high pressures, whereas the same reaction for ferrocene in solution is not. The reduction of ferrocenium back to ferrocene was found to be affected to a lesser degree by pressure. Positive volumes of reaction and activation, indicative of a volume expansion, were found to be associated with the oxidation of ferrocene in the SAM. This volume increase, on the order of $10-20$ cm^3 mol^{-1}, is attributable to the surface confinement of the ferrocene moiety which requires a reorganization of the $Fc^+C_{11}SAu$ SAM to allow for the complexation of perchlorate counterions.[104] Such a volume expansion would produce an internal film pressure of ca. $0.1-0.2$ GPa[123] and result in bending of the $FcC_{11}SAu$ microcantilever away from the Au-coated face, as observed in our experiments.

Surface spectroscopic investigations of FcRSAu SAMs support the notion of a ferrocene-oxidation-induced monolayer reorganization. Recent ellipsometry[77,92,124] and surface plasmon resonance spectroscopy (SPR)[100,125] investigations of FcRSAu SAMs report a thickening of the monolayer film (Δd) by $0.1-0.3$ nm upon oxidation of the terminal ferrocene moieties. Such an increase in film thickness translates into a volume change ($= \Delta d \times 4.5 \times 10^{-10}$ mol cm^{-2}), $\sim 20-70$ cm^3 mol^{-1}, that is of similar magnitude to that reported by Cruañes et al.[104] Cruañes et al. originally proposed a stretching of the surface-tethered ferrocenylalkylthiolate alkyl chains to facilitate the association of the ferrocenium cations with perchlorate counterions.[104] Fourier transform infrared reflection absorption spectroscopy (FT-IRRAS) indicates that the observed changes in film thickness arise from a molecular orientational change in the SAM, resulting in either the alkyl chains[83,84] or cyclopentadiene rings[77,82] adopting a more perpendicular orientation with respect to the surface normal. A more recent in situ Fourier transform surface-enhanced Raman spectroscopy (FT-SERS) study of FcC_4COOC_nSAu SAMs, suggests that ferrocene oxidation causes the alkyl chains to adopt a more perpendicular orientation with respect to the electrode surface.[70] The ferrocenium-bearing alkyl chains and ferrocenium cyclopentadiene rings can change their orientation, to allow for the complexation of perchlorate counterions (Figure 7).[69,70,76,82−84,126−128] More importantly, the proposed molecular reorientation could only occur in a concerted (as opposed to isolated) movement. The molecular reorientation/monolayer volume expansion would

(118) The apparent dipole moment of an alkanethiolate-Au monolayer is composed of contributions from $Au^{\delta+}-S^{\delta-}$ and from $S^{\delta-}-R^{\delta+}$ (see ref 119), where the partial charge on the S determined by X-ray photoelectron spectroscopy is ~ -0.2e (see ref 120). Formation of the ion pair will increase the apparent molecular dipole moment and the magnitude of the associated repulsive dipolar forces between the alkanethiolate molecules. Such dipolar repulsive forces have already been identified as being the source of the compressive surface stress changes observed during the self-assembly of *n*-alkanethiols on gold-coated microcantilevers (see ref 30).

(119) Evans, S. D.; Ulman, A. *Chem. Phys. Lett.* **1990**, *170*, 462–466.
(120) Bourg, M.-C.; Badia, A.; Lennox, R. B. *J. Phys. Chem. B* **2000**, *104*, 6562–6567.
(121) Hudson, J. E.; Abruña, H. D. *J. Am. Chem. Soc.* **1996**, *118*, 6303–6304.
(122) Noy, A.; Vezenov, D. V.; Lieber, C. M. *Annu. Rev. Mater. Sci.* **1997**, *27*, 381–421.
(123) These values were obtained through a rough calculation using the ideal gas law with a molar volume change of $10-20$ cm^3 mol^{-1} and $T = 295$ K.
(124) Abrantes, L. M.; Kalaji, M.; Viana, A. S. *Russ. J. Electrochem.* **2002**, *38*, 39–43.
(125) Yao, X.; Wang, J.; Zhou, F.; Wang, J.; Tao, N. *J. Phys. Chem. B* **2004**, *108*, 7206–7212.
(126) The packing density of the ferrocenylundecanethiolates restricts the redox-induced folding of the ferrocene-terminated alkanethiolates, so that direct interaction of the ferrocenes with the underlying Au surface is unlikely, except at grain boundaries and defect sites (see refs 127 and 128).
(127) Wang, X.; Kharitonov, A. B.; Katz, E.; Willner, I. *Chem. Commun.* **2003**, 1542–1543.
(128) Lahann, J.; Mitragotri, S.; Tran, T.-N.; Kaido, H.; Sundaram, J.; Choi, I. S.; Hoffer, S.; Somorjai, G. A.; Langer, R. *Science* **2003**, *299*, 371–374.

result in an expanding lateral tension that could drive the microcantilever deflection reported herein.

As mentioned in the Introduction, mechanical actuation based on redox-induced volume changes is a well-known phenomenon in conducting polymer film systems. We therefore attribute a redox-induced SAM volume expansion, brought about by collective molecular reorientations, as the most likely source of the surface stress changes measured for the $FcC_{11}SAu$ cantilevers. A comparison of the results reported for polyaniline-[49] and polypyrrole-[50]coated microcantilevers with those obtained for the $FcC_{11}SAu$-modified microcantilevers reveals that the surface stress change per charge density generated by the monomolecular (1.8 nm thick)[100] $FcC_{11}SAu$ (4500 N m^{-1}/C cm^{-2}) is significantly greater than the stresses of the thicker multilayer polymer films: ~300 N m^{-1}/C cm^{-2} (polyaniline; 190 nm thick)[86,87] and ~20 N m^{-1}/ C cm^{-2} (polypyrrole; 300 nm thick).[88] The larger stress change observed for the $FcC_{11}SAu$ microcantilever is probably due to the greater steric constraints in the closer-packed $FcC_{11}SAu$ SAM compared to the conducting polymer films and an efficient coupling between the chemisorbed $FcC_{11}S-$ monolayer and the Au-coated microcantilever transducer vs the physisorbed polyaniline and polypyrrole. Although larger deflections are theoretically obtainable by building thicker films of conducting polymers (i.e., increase the number of redox sites per square area), the charge-normalized surface stress of the $FcC_{11}SAu$ SAM demonstrates that other system properties can be tailored to produce a larger actuation. Finally, our results point to ferrocenylalkanethiolate SAMs as potentially promising electroactuating coatings in such applications as nanomechanics, nanotweezers, and micromechanical elements, where there is a strong preference for actuation in a constant chemical environment.

Conclusions

We demonstrate that the surface stress changes associated with the oxidation and subsequent reduction of an electroactive moiety confined at an organic monolayer/solution interface can induce a reversible micromechanical motion. While SAM-modified microcantilevers often exhibit small nanometer-scale deflections, the electrochemical oxidation of $FcC_{11}SAu$ generates maximum deflections that approach the micrometer scale for cantilevers with a low spring constant (0.01 N m^{-1}). The significance of this work is that it demonstrates that electroactive self-assembled monolayer films of well-defined structure can be used for micromechanical actuation.

Our results are consistent with the redox-induced deflection of a $FcC_{11}SAu$ microcantilever being predominantly driven by a monolayer volume expansion resulting from collective reorientational motions caused by the complexation of perchlorate ions to the surface-immobilized ferroceniums. The cantilever responds to the lateral pressure exerted by an ensemble of reorienting ferrocenium-bearing alkylthiolates upon each other rather than to individual anion pairing events, resulting in a complex nonlinear dependence of the cantilever deflection on the quantity of electrogenerated ferrocenium (i.e., Figure 5B). Our work suggests that steric constraints and/or the ability of the complexing ion to induce organizational changes within the monolayer film play an important role in the magnitude of the observed cantilever bending in redox-induced actuation. We believe that this finding is not limited to ferrocene-terminated monolayers, and that SAM-modified cantilevers generally respond to collective in-plane molecular interactions rather than reacting to single (bio)chemical events. This notion is based on literature examples of other types of interfacial reactions at SAMs being affected by steric crowding of the terminal functional groups (e.g., pK_a/pK_b of acid−base groups,[129] binding capacity of proteins,[130] and DNA−drug binding affinity[131]). The steric crowding of the reactive termini is imposed by the packing density of the ω-functionalized alkanethiolates and is present to various extents in all SAMs, so that a molecular rearrangement of the alkanethiolates within the SAM is expected for the (bio)chemical reaction to proceed.

In an effort to further understand the fundamental mechanisms of surface stress in ferrocenylalkanethiolate SAMs, we will continue to investigate the response of modified microcantilevers as a function of chemical structure and molecular order as well as anion-pairing strength. These experimental variables should provide further dynamic control over both the magnitude and direction of microcantilever deflection. In view of potential applications, an evaluation of the mechanical actuation performance of ferrocenylalkanethiolate-modified cantilevers upon repeated redox cycling and under prolonged potential holds will be undertaken by our laboratory.

Acknowledgment. This work was supported by NSERC (Canada), CFI (Canada), FQRNT (Québec), the Canada Research Chairs program, and the Université de Montréal. L.N. gratefully acknowledges fellowship support from the Groupe de recherche en technologie des couches minces of the Regroupement québécois sur les matériaux de pointe. We thank Mr. Jean-François Myre and Mr. Louis Beaumont (Chemistry Mechanics and Electronics Shop, Université de Montréal) for their contributions to the microcantilever optical deflection setup. We would also like to thank Brian Seivewright (McGill University) and Jeff Shepherd (Laurentian University) for their help with the software programming used for data collection.

Supporting Information Available: Experimental details and additional results. This information is available free of charge via the Internet at http://pubs.acs.org.

JA808400S

(129) Fears, K. P.; Creager, S. E.; Latour, R. A. *Langmuir* **2008**, *24*, 837–843.
(130) Spinke, J.; Liley, M.; Schmitt, F. J.; Guder, H. J.; Angermaier, L.; Knoll, W. *J. Chem. Phys.* **1993**, *99*, 7012–7019.
(131) Wolf, L. K.; Gao, Y.; Georgiadis, R. M. *J. Am. Chem. Soc.* **2007**, *129*, 10503–10511.